Dry surface biofilm of *Salmonella* and *Cronobacter sakazakii*: a real concern for the low moisture food industry

Vinícius S. A. Vaz[a#], Jéssica de A.F.F. Finger[a#], Raul F. Pereira[a], Mariana S. Derami[a], Jean-Yves Maillard[b], Maristela S. Nascimento[a*]

[a]Departamento de Engenharia e Tecnologia de Alimentos, Faculdade de Engenharia de Alimentos, Universidade Estadual de Campinas, Unicamp, Campinas, SP, Brasil.

[b]School of Pharmacy and Pharmaceutical Sciences, Cardiff University, Cardiff, UK.

[#]These authors contributed equally.

[*]**Corresponding author:** Maristela S. Nascimento, Departamento de Engenharia e Tecnologia de Alimentos, Faculdade de Engenharia de Alimentos, Universidade Estadual de Campinas, Unicamp, Rua Monteiro Lobato n° 80, Campinas, São Paulo, 13083-862, Brasil. E-mail address: mnasci@unicamp.br.

Abstract

Salmonella and *Cronobacter sakazakii* have been associated with outbreaks linked to low-moisture foods (LMF). Their persistence under desiccation stress can contribute to biofilm formation. This study evaluated different dry surface biofilm (DSB) formation protocols on stainless steel (SS) and polypropylene (PP), which differ with the combination of their hydrated (from 24 to 48h) and dry phase (from 48 to 120h). For *Salmonella*, cultivable sessile cells (CSC) and viable sessile cells (VSC; corresponding to CSC and viable but non-culturable (VBNC) cells) reached up to 7.2 and 8.6 log CFU/cm², respectively, while *C. sakazakii* exhibited higher concentrations, up to 8.1 log CFU/cm² (CSC) and 9.0 log CFU/cm² (VSC). A combination of 8h wet + 120h dry phases resulted in the lowest counts ($p < 0.05$), with CSC ranging from 3.7 to 5.5 log CFU/cm² for *Salmonella* and 4.5 to 6.3 log CFU/cm² for *C. sakazakii*. The duration of the wet phase was the main factor influencing DSB formation. The lowest difference between CSC and VSC (1.1 and 0.6 log CFU/cm² respectively) was noted with a combination of 24h wet + 72h dry phases, whereas the largest difference (2.8 and 2.2 log CFU/cm² for *Salmonella* and *C. sakazakii,* respectively) occurred with the combination of 8h wet + 120h dry phases. Confocal laser scanning microscopy showed the DSB thickness was impacted by the DSB formation protocol: from 10.4-12.7 µm thickness with a combination of 48h wet + 48h dry phases or 24h wet + 120h dry phases, 3.3–7.1 µm with a combination of 24h wet + 72 h dry phases. Morphological changes such as elongation, spherical shape, desiccation, and cell lysis were observed in all biofilms. Regardless of the protocol used, both bacteria were able to form DSB with the presence of VBNC cells, highlighting the importance of strict moisture control and effective sanitation in LMF plants.

Keywords: Food safety; biofilm; low-moisture food; hygiene.

1. Introduction

Biofilms are complex microbial communities, composed of either a single species or multiple, and are adhered on abiotic or biotic surfaces (Sadiq et al., 2023). They may or may not be embedded in a matrix composed of a wide variety of extracellular polymeric substances (EPS) (Karygianni et al., 2020; Sadiq et al., 2023; Sauer et al., 2022). Biofilms pose a major public health concern due to their remarkable capacity for dissemination and survival under adverse environmental conditions, displaying resistance to physical, chemical, and mechanical agents (Dallal et al., 2023; Lories et al., 2020). Consequently, they are estimated to have a global economic impact of approximately US$5 trillion (Cámara et al., 2022), affecting sectors such as agriculture (Rodrigues et al., 2008), maritime transport (Akuzov et al., 2013), water quality and safety (Learbuch et al., 2019), the food industry (Alonso et al., 2023; Alvarez-Ordóñez et al., 2019; Galié et al., 2018) and healthcare (Abdallah et al., 2014; Weber et al., 2023). In the food industry, biofilms lead to economic losses due to product spoilage and are also linked to outbreaks of foodborne diseases (Dass and Wang, 2022). However, most studies are focusing on hydrated (wet) biofilms, and little is known on biofilm grown in dry environment. The presence of Dry Surface Biofilms (DSB) was first reported in Australia in the medical setting, and revealed the persistence of *Staphylococcus aureus* biofilms on dry hospital surfaces (Vickery et al., 2012). Since then, DSB have been widely reported in healthcare settings (Almatroudi et al., 2016; Chowdhury et al., 2018; Ledwoch et al., 2018; Ledwoch et al., 2019). While the term DSB was coined in 2015 (Almatroudi et al., 2015), there is not yet an official definition of DSB. Nevertheless, according to Ledwoch et al. (2022) DSB are biofilms present in a desiccated state on environmental surfaces exposed to low-moisture conditions. In general, DSB tend to be thinner, have a more heterogeneous distribution across surfaces and have thinner EPS when compared to hydrated biofilms (Ledwoch et al., 2022). In addition, DSB are not reliably detected by conventional wet-swabbing procedures and exhibit greater resistance to disinfection than biofilms formed under hydrated condition (Almatroudi et al., 2015; Ledwoch et al., 2018).

In the low-moisture food (LMF) processing environment, DSB can represent a significant risk of contamination (Chaggar et al., 2024); pose an additional challenge for microbiological control and food safety management

(Alonso et al., 2023). Studies have shown that foodborne pathogens, such as *Salmonella* spp. (Anderson et al., 2017; Ly et al., 2019; Maćkiw et al., 2024) and *Cronobacter sakazakii* (Beuchat et al., 2013; Sawale et al., 2022), can survive for prolonged periods in LMF, such as infant formula, chocolate, cereals, flour, pasta, and spices; as well as in food processing environments (Amaeze et al., 2024; Liu et al., 2022; Ly et al., 2019). It has also been shown that *Salmonella* spp. can form DSB on different surfaces, although direct comparisons between surfaces are lacking. Chaggar et al. (2024) observed DSB formation on borosilicate glass coupons, while Duggan et al. (2024) reported that *Salmonella* Typhimurium DSB are less susceptible to disinfection than hydrated biofilms. Likewise, Lin et al. (2024) demonstrated that *Salmonella* Typhimurium DSB exhibits greater tolerance to sanitization compared to biofilms formed on moist surfaces. The ability of *C. sakazakii* to form DSB has not been reported, nor its behavior on different surfaces.

Fluctuation between high and low water activity as observed in a LMF processing plant after sanitation can drive bacterial adaptative response, leading to a greater tolerance and biofilm formation (Eriksson de Rezende et al. 2001). In addition bacteria can enter a Viable But Non-Culturable (VBNC) state due to stress conditions (starvation and desiccation) (Chen et al., 2021). VBNC state is characterized as cells that lose their culturability on nutrient media while maintaining the metabolic activity, including their virulence potential, and their membrane integrity. However, VBNC cells can be resuscitated under favorable conditions (Truchado et al., 2023; Zhang et al., 2021). Catalase has been successfully used to resuscitate VBNC cells (Abdelhamid and Yousef, 2020; Ma et al., 2024; Morishige et al., 2017). Catalase is crucial for counteracting oxidative stress and resuscitating cells from a non-culturable to a culturable state (Borisov et al., 2021; Morishige et al., 2017). In general, VBNC cells exhibit increased tolerance to sanitizing agents such as chlorine-based and quaternary ammonium compounds (Highmore et al., 2018), which makes them particularly relevant for food processing environments. This poses a significant challenge for existing cleaning and disinfection protocols, as routine monitoring may under estimated the bacterial population (Chen et al., 2021). Although VBNC induction has been documented under desiccation and sanitizer exposure, and a significant fraction of DSB population may exist in the VBNC state Lin et al. (2024), no study has

specifically quantified VBNC cells within DSB formed by foodborne pathogens.

Currently, there is no standard methodology for DSB formation. The first experimental model described by Almatroudi et al. (2015) was based on the use of the CDC reactor alternating successive hydrated and dry phases every 48h for 12 days. The CDC reactor approach has been used by others (Chaggar et al., 2024), while a sedimentation biofilm approach also using successive hydrated and dry phases for 12 days has been adopted by Maillard's group in Wales (Centeleghe et al., 2023; Ledwoch et al., 2018; Ledwoch et al., 2019). Other DSB formation protocols have been reported with the aim to mimic better the environment (Esther et al. 2023; Lin et al., 2024). Hydrated–dry cycle combinations also varied depending on the study, ranging from a single cycle (Chaggar et al., 2024) to two (Lin et al., 2024), three (Ledwoch et al., 2019), or even four cycles (Almatroudi et al., 2015; Rahman et al., 2022). The duration of each phase also differs considerably, with hydrated phases lasting from 6 to 48 h and dry phases extending up to 72 h (Almatroudi et al., 2015; Chaggar et al., 2024; Ledwoch et al., 2018; Lin et al., 2024). Variation in methodology influences the type and extent of DSB formation, making direct comparisons difficult.

In this context, the present study aims to evaluate the ability of *Salmonella* spp. and *C. sakazakii* to form DSB on stainless steel (SS) and polypropylene (PP) coupons, materials commonly used in the food industry. In addition, we investigated the presence of the VBNC state, morphological changes in bacterial cells, and the spatial dimension of these biofilms.

2. Materials and methods

2.1 Bacterial strains and preparation of inocula

Four *Salmonella* spp. strains, isolated from the peanut production chain in Brazil, and five strains of *C. sakazakii* isolated from LMF processing environment were used in this study (Table 1). All *C. sakazakii* and *Salmonella* strains demonstrated their ability to form a biofilm under hydrated conditions (Umeda et al., 2017; von Hertwig et al., 2022).

Table 1. Details about *Salmonella* spp. and *C. sakazakii* strains.

Code	Source of isolation	Identification	Reference and/or source
***Salmonella* spp.**		Serovar	
P03.2 FEA	Peanuts (primary production)	Muenster	Nascimento et al (2018) and von Hertwig et al (2019)
P6.1 FEA	Peanuts (processing)	Javiana	
P07.1 FEA	Peanuts (processing)	Oranienburg	
P10.5 FEA	Peanuts (primary production)	Miami	
C. sakazakii		Biogroup	
P4499	Milk powder	8a	INCQS[a]
P4787	Pre-cooked rice-based cereal	2	
P4791	Ground ginger	3	
P4795	Rice / oat cereal mix	1	
P4798	Breadcrumbs	5	

[a]Strain bank of the National Institute for Quality Control in Health (INCQS) of the Oswaldo Cruz Foundation, Rio de Janeiro, RJ, Brazil.

Salmonella spp. and *C. sakazakii* strains were stored in a -80 °C ultra-low temperature freezer. For reactivation, a glass bead containing the microorganism was transferred to 5 mL of Brain Heart Infusion (BHI; Difco, Sparks, MD, USA) and incubated at 37 °C for 18-20 h. Subsequently, the strains were streaked onto slanted Trypticase Soy Agar (TSA; Difco, Sparks, MD, USA), incubated again at 37 °C for the same duration; and then stored at 4 °C for further use.

At the time of the experiment, the strains underwent two successive subcultures in BHI, with incubation at 37 °C for 18-24 h for each passage. Following this process, strains were again streaked onto TSA and incubated for 24 h at 37 °C. A loopful of each strain was then transferred to tubes containing 0.85% saline solution (Synth, Brazil), and turbidity adjusted to 0.5 on the McFarland scale. Decimal dilutions were prepared in 0.1% peptone water (Difco, Sparks, MD, USA) and subsequently inoculated into Tryptic Soy Broth (TSB;

166 Difco, Sparks, MD, USA) to achieve a final concentration of approximately 6 log
167 CFU/mL (Test suspension).
168
169 **2.2 Preparation of the coupon**
170 To assess adhesion and dry biofilm formation of *Salmonella* spp. and *C.*
171 *sakazakii*, SS and PP coupons measuring 1 cm² were used. Prior to each
172 experiment, the coupons underwent a cleaning procedure adapted from Rosado
173 (2009). First, coupons were subjected to an ultrasonic bath (Ultronique, Brazil)
174 for 15 min at 40 kHz. Next, coupons were immersed in an anionic surfactant
175 detergent solution, manually scrubbed, and rinsed with distilled water. They were
176 then immersed in 70% ethanol for 2 h, followed by another rinse with distilled
177 water. Finally, the cleaned coupons were sterilized at 121 °C for 30 min.
178
179 **2.3 DSB formation**
180 Five distinct protocols (T1-T5) were evaluated for the formation of DSB.
181 Each protocol consisted of two consecutive cycles, and each cycle included a
182 hydrated phase followed by a dry phase (Table 2).
183
184 **Table 2.** DSB **formation** protocols.

Microorganism	Protocol number	Incubation time (h)				
		Cycle 1		Cycle 2		Total period *
		Wet phase	Dry phase	Wet phase	Dry phase	
Salmonella spp. and *C. sakazakii*	T1	48	48	48	48	192
Salmonella spp.	T2#	24	48	24	48	144
Salmonella spp. and *C. sakazakii*	T3	24	72	24	72	192
Salmonella spp. and *C. sakazakii*	T4	24	120	24	120	288
Salmonella spp. and *C. sakazakii*	T5	8	48	8	48	112

*After two sequential DSB formation cycles.

Protocol T2 (24 h wet + 48 h dry) was evaluated exclusively for *Salmonella* spp. and not for *C. sakazakii*.

The DSB formation protocols were established based on varying exposure times to moisture and water restriction, simulating typical conditions found in food processing environments. Each cycle consisted of one hydrated phase followed by one dry phase, and each protocol comprised two cycles (adapted from Ledwoch et al., 2019). SS and PP coupons were placed in flat-bottom 24-well plates (Costar®, Kennebunk, ME, USA) and inoculated with 1 mL of TSB containing the *Salmonella* spp. and *C. sakazakii* test suspensions (section 2.1). The coupons were then incubated at room temperature under gentle agitation using an Orbit P2 shaker (Labnet International, Edison, NJ, USA) for 8, 24, or 48 h, characterizing the hydrated phase of cycle 1. After this period, the culture medium was carefully removed using a micropipette, and the plates were incubated at 25 °C under static conditions for 48, 72, or 120 h, corresponding to the dry phase of cycle 1. After that, 1 mL of TSB solution only was added to the wells and incubated as described above for the first hydrated phase of cycle 2. After 8, 24, or 48 h, all media was drained out, and the plates were incubated for an additional 48, 72, or 120 h at 25 °C under static conditions, corresponding to the dry phase of cycle 2.

2.3.1 Microbial quantification

After each cycle, counts of cultivable sessile cells (CSC) and VBNC cells were determined. Total viable sessile count (VSC) represents the sum of CSC and VBNC cells.

Coupons were transferred to tubes containing 10 mL of 0.85% saline solution and left in contact for 30 s to remove planktonic cells. Each coupon was then transferred to a tube containing 5 mL of 0.85% saline solution and 10 glass beads, followed by vortexing for 1 min (adapted from Ziech et al., 2016). Subsequently, decimal dilutions were prepared and plated on TSA, followed by incubation at 37 °C for 24 h to determine CSC.

To recover VBNC cells, 1 mL of the 0.85% saline solution was transferred to tubes containing 1 mL of minimal medium (M9 broth without glucose; Sigma,

St. Louis, MO, USA) supplemented with 10,000 U of bovine liver catalase (Sigma, St. Louis, MO, USA) and incubated at 37 °C for 6 h. After incubation, the solution was plated on TSA and incubated at 37 °C for 24 h (Morishige et al., 2017). Results were expressed as log CFU/cm².

2.4 Scanning Electron Microscopy (SEM)

For SEM analysis, one coupon from each DSB formation protocol was immersed in 10 mL of 0.85% saline solution for 30 s to remove planktonic cells. The coupons were then fixed in 2 mL of 0.1 M phosphate buffer solution supplemented with 2% glutaraldehyde for 3 h. After this period, the coupons were washed twice with 0.1 M phosphate buffer and subjected to a gradual dehydration process using analytical grade ethanol, as described by Lou et al. (2013).

To remove alcohol completely, the coupons were transferred to a Critical Point Dryer (Balzers, model CPD-030, Liechtenstein), using carbon dioxide as the transitional agent. Subsequently, the coupons were coated with gold for 180 s using a Sputter Coater (Balzers, model SCD-50, Liechtenstein) and analyzed using a Scanning Electron Microscope (ThermoFisher Scientific, Quattro S, Czech Republic).

2.5 CLSM analysis

The spatial distribution and topography of biofilms were analyzed using Confocal Laser Scanning Microscopy (CLSM) with the FilmTracer™ LIVE/DEAD® Biofilm Viability Kit (Invitrogen, Eugene, OR, USA) at a 1:1000 dilution. The fluorophores SYTO® 9 and propidium iodide were excited/emitted at 482/500 nm and 490/635 nm, respectively. At the end of each DSB formation protocol, one SS and one PP coupon were stained for 10 min, washed with PBS, and kept in the dark until image acquisition. DSB samples were imaged using a Zeiss LSM780-NLO confocal microscope coupled to an Axio Observer Z.1 microscope (Carl Zeiss AG, Germany), equipped with a 40×/0.6 water-immersion objective.

Three-dimensional reconstruction, as well as analysis of the topography and spatial distribution of DSB cells, was performed using FIJI software (ImageJ, https://imagej.net/ij/index.html). Three-dimensional images were acquired in separate channels for each fluorophore, using Z-stack mode with ~1.4 µm

spacing between planes throughout the entire depth of the biofilm, over a scanning area of 212 x 212 µm. Biofilm thickness was determined by visualization in the ZY plane, based on 1.4 µm intervals, according to a methodology adapted from Capita et al. (2019). Measurements were taken at three points along the Y-axis (30 µm, central region ~106 µm, and 180 µm), centered on the X-axis. The Z-axis represented the depth (µm). Thickness was expressed as the mean ± standard deviation. For topographic analysis, images were rendered in 3D with superimposition of the Z-stack planes. The X and Y axes represent the scanned area (µm), while the Z-axis indicates luminance, corresponding to the intensity of the fluorescent signal. The COMSTAT2 program (www.comstat.dk, Heydorn, 2000; Vorregaard, 2008) was used to evaluate the maximum biofilm thickness (µm) and biofilm biomass (µm²/µm³) obtained from each channel (green/red). The COMSTAT2 was used as a plugin in ImageJ (https://imagej.net/ij/).

2.6 Statistical analysis

Each experiment was performed in three independent replicates. The CSC and VSC counts were analyzed by one-way ANOVA and Tukey's test to determine the influence of DSB protocols, surface materials and DSB cycle number on these parameters ($p \leq 0.05$) Statistical analyses were performed using the Statistical Analysis System software (SAS v.9.4, Cary, NC, USA).

3. Results

3.1 DSB enumeration

In this study, the biofilm-forming capacity of DSB by *Salmonella* spp. and *C. sakazakii* on SS and PP coupons was evaluated. Five DSB formation protocols were tested for *Salmonella* spp., and four for *C. sakazakii*. Each protocol consisted of two hydration and dehydration cycles with varying durations (Table 2).

For *Salmonella*, no significant difference ($p > 0.05$) was observed between cycle 1 and cycle 2 for both CSC (catalase non-treated) and VSC (catalase-treated) counts. There were no significant differences in CSC or VSC ($p > 0.05$) on SS between T1 and T4 DSB protocols. By the end of cycle 2, CSC counts reached 6.5 log CFU/cm² for T1, 6.7 log CFU/cm² for T2, 6.8 log CFU/cm² for T3,

6.5 log CFU/cm² for T4, but only 3.7 log CFU/cm² for T5. A significant difference in CSC and VSC ($p < 0.05$) was detected on PP between T3-cycle 2 and T5-cycle 2, with counts of 7.2 and 5.0 log CFU/cm², respectively, while CSC and VSC counts following cycle 2 from other protocols were around 6.5 log CFU/cm². In addition, for this cell group, a significant difference ($p < 0.05$) between surfaces was observed for T5 (3.7 log CFU/cm²) on SS-cycle 1 and SS-cycle 2 compared top 5.5 log CFU/cm² on PP-cycle 1.

Catalase treatment led to a significant increase ($p < 0.05$) in the biofilm population recovered on both surfaces, suggesting the presence of VBNC state. On SS, the lowest VSC count was noted for T5 (5.9–6.5 log CFU/cm²), whereas other protocols ranged from 7.7 to 8.6 log CFU/cm². There was a significant difference in VSC ($p < 0.05$) between T5-cycle 1 and cycle 1 or cycle 2 for other protocols. On PP, there was no significant difference ($p > 0.05$) in VSC counts (ranging from 7.4 to 8.3 log CFU/cm²). There was no significant difference ($p > 0.05$) in VSC count from T5 between PP and SS, despite the observed 1.5 log difference in number. The greatest raise in the DSB population after catalase resuscitation were obtained for T5-cycle 2 (2.4 log CFU/cm² on PP and 2.8 log CFU/cm² on SS), whereas other protocols ranged from 1.1 to 1.9 log CFU/cm².

There was no significant difference in CSC or VSC for *C. sakazakii* between both cycles for any protocol ($p > 0.05$). The lowest CSC count was observed in T5-cycle on SS (4.5 log CFU/cm²), and the highest in T3-cycle on SS (8.1 log CFU/cm²). CSC from other protocols ranged from 6.3 to 7.6 log CFU/cm². There was no significant difference ($p < 0.05$) only between T5-C1-SS and all other protocols, except T1-C2-SS.

Regarding the surface material, there was significant difference ($p < 0.05$) only between T5-C1-SS and T5-C2-PP, 4.5 log CFU/cm² versus 7.1 log CFU/cm². For VSC, no significant differences ($p > 0.05$) were detected among protocols or surfaces. The counts ranged from 7.2 to 9.0 log CFU/cm² on SS and from 8.3 to 8.7 log CFU/cm² on PP. The highest increase in the DSB counts after catalase treatment was observed for T5-C1-SS (2.7 log CFU/cm²), followed by T5-C1-PP and T1-C2-SS (2.2 log CFU/cm²), whereas T3-C1-SS exhibited the smallest value (0.6 log CFU/cm²), and all other protocols ranged from 1.0 to 1.9 log CFU/cm².

3.2 DSB cell morphology

Phenotypic changes in the morphology of both bacterial species were observed. The most frequently observed phenomena included cell elongation and filamentation, the latter distinguished by the presence of visible septa within long-chain cell structures (Figures 3 and 4, yellow arrow). Furthermore, many cells exhibited coccoid morphology (Figure 3 and 4, blue arrow) or signs of reduced turgor, as evidenced by cell shrinkage or wilting (Figure 3 and 4, red arrow). Membrane rupture was also verified in some cells, indicating possible cell lysis (Figure 3 and 4, orange arrow). In addition, these morphological alterations were more frequently observed in *Salmonella* DSB. SEM images revealed the formation of bacterial biofilms, with the production of an EPS matrix (Figures 3 and 4, green arrow) on both SS and PP coupons across all DSB formation protocols evaluated.

3.3 CLSM analysis

The analyses of the CLSM images revealed that the thickest *Salmonella* DSB were observed on PP, with T1 (12.7 ± 2.3 µm) followed by T4 (9.4 ± 0.7 µm). On SS, the highest average values were for T1 and T2 (both 8.5 ± 1.2 µm). The densest biofilms were found in T3 on PP (3.3 ± 0.7 µm) and in T5, 4.7 ± 0.7 µm on SS and 4.2 ± 1.2 µm on PP (Table 3). For *C. sakazakii*, the variation in DSB thickness across protocols was less pronounced. The greatest average thickness values were recorded in T4 on PP and T1 on SS, both measuring 10.4 µm (Figures 7 and 8). The lowest values were observed in T3, 5.7 ± 0.2 µm on PP and 7.1 ± 1.2 µm on SS. On the other hand, the maximum thickness was more similar among *Salmonella* than *C. sakazakii* DSB protocols, except in T5 (Table 3). In terms of spatial distribution, DSB formed on SS were generally more homogeneous than those on PP for both bacterial species (Figure 5 and 6). The biomass of live (green signal) and dead (red signal) cells did not follow a standard pattern (Supp. 1). For *Salmonella* T1, T2 and T3 showed a higher percent of dead cells on SS, whereas in T4 and T5 this predominance occurred on PP (Table 3). In contrast, the opposite was noted for *C. sakazakii.*

355 **Table 3.** Characterization of DSB formed by *Salmonella* and *C. sakazakii* in SS
356 and PP surfaces.

Inoculum	DSB protocol	Surface material	Thickness (µm)		Cell biomass (µm³/µm²)[3]	
			Average[1]	Maximum[2]	% Dead cells (red)	% Live cells (green)
Salmonella	T1	PP	12.7 ± 2.3	15.6	29.4	70.6
		SS	8.5 ± 1.2	9.9	50.5	49.5
	T2	PP	6.1 ± 0.7	15.6	14.6	85.4
		SS	8.5 ± 1.2	15.6	43.8	56.2
	T3	PP	3.3 ± 0.7	14.1	7.8	92.2
		SS	6.8 ± 2.0	15.6	44.7	55.3
	T4	PP	9.4 ± 0.7	15.6	38.5	61.5
		SS	6.6 ± 1.3	15.6	9.0	91.0
	T5	PP	4.2 ± 1.2	9.9	61.6	38.4
		SS	4.7 ± 0.7	9.9	32.7	67.3
C. sakazakii	T1	PP	9.6 ± 0.4	9.7	56.0	44.0
		SS	10.4 ± 0.7	14.1	31.1	68.9
	T3	PP	5.7 ± 2.0	17.0	46.5	53.5
		SS	7.1 ± 1.2	22.6	25.8	74.2
	T4	PP	10.4 ± 1.8	15.6	48.1	51.9
		SS	9.7 ± 2.9	15.6	71.0	29.0
	T5	PP	7.5 ± 1.3	15.5	27.9	72.1
		SS	9.1 ± 1.0	12.7	40.1	59.9

T1 – 48 h wet + 48 h dry; T2 – 24 h wet + 48 h dry; T3 – 24 h wet+ 72 h dry; T4 – 24 h wet + 120 h dry; T5 – 8 h wet + 48 h dry. [1]Values are arithmetic mean with a standard deviation of three replicates. [2]Calculated using COMSTAT2. [3]Cell biomass = Biomass of live or dead cells/ (Biomass of live cells + Biomass of dead cells), calculated using COMSTAT2.

357 **4. Discussion**

358 This is the first study to evaluate different conditions for DSB formation by
359 *Salmonella* and *C. sakazakii* strains, isolated from LMF processing environments,

on surfaces commonly used in the food industry (SS and PP). This study also investigated the presence of VBNC cells in DSB. The experimental protocols were adapted from Ledwoch et al. (2019), with each DSB protocol comprising two hydrated and dry cycles, as detailed in Table 2. Whilst we did not use any bovine serum albumin (BSA) in the hydrated phase, which helped with the viability of *Staphylococcus aureus* during DSB formation (Ledwoch et al., 2019), CSC obtained in most our protocols were > 6 log CFU/cm². These counts were similar to the *Salmonella* Typhimurium counts reported by Duggan et al. (2024) who used six wet-dry cycles over a period of 12 days and BSA in each hydrated phase.

The majority of *Salmonella* DSB protocols (T1 to T4) resulted in CSC counts between 6 and 7 log CFU/cm², reaching up to 8.6 log CFU/cm² after catalase resuscitation (VSC, Figure 1). Chaggar et al. (2024) reported similar results with counts from 6.3 to 7.1 log CFU/coupon for *S.* Typhimurium ATCC 14028 biofilms on borosilicate glass, using a 24-h hydrated phase followed by dehydration for 24, 48, and 72 h. Lin et al. (2024) also evaluated *S.* Typhimurium ATCC 14028 DSB formation on Petri dishes under a single condition (48 h wet + 48 h dry + 6 h wet + 66 h dry) and reported approximately 6.0 log CFU/plate. In addition, T5 (8-h wet + 48-h dry) yielded the lowest counts, with a significant difference ($p < 0.05$) compared with other protocols, especially on SS (Figure 1). This suggests that the duration of moisture exposure plays a crucial role in the *Salmonella* DSB formation on abiotic surfaces, while water restriction during the dry phase has a lesser impact on the number of cells. It is well known that desiccation stress induces molecular defense responses in the *Salmonella* cells, including the accumulation of trehalose and other compatible solutes, along with synthesis of stress proteins such as heat-shock proteins and chaperones (Gruzdev et al., 2012; Wang et al., 2021). Nonetheless, there is a lack of data on the molecular mechanisms involved in DSB formation and persistence. Notably, *C. sakazakii* exhibited CSC counts up to 1.0 log CFU/cm² higher than those observed for *Salmonella* in T1, T3 and T4, and > 2 log CFU/cm² in T5 (Figure 1 and 2). It suggests a greater adaptability capacity of this pathogen to conditions of nutrient and water restrictions, as well as a greater rate of biofilm formation. However, to date, no published studies have addressed DSB formation or persistence by *C. sakazakii*, limiting direct comparisons. The ability of *C.*

sakazakii to survive in powdered infant formula (PIF) for extended periods and its association with severe infections in neonates have been reported (Beuchat et al., 2013; FAO/WHO, 2006; Strysko et al., 2020). Indeed, our results have critical implications for PIF manufacturing plants, since evidence that the presence of DSB can increase the risk of cross-contamination in final product. Another noteworthy finding is the ability of both pathogens to form DSB even after a single exposure to high humidity (cycle 1, Figure 1 and 2). In fact, accidental leaks or residual moisture post-sanitation can suffice to initiate biofilm formation. These results align with the Code of Hygienic Practices for LMF of Codex Alimentarius (CXC 75-2015, 2018), which recommends strict humidity control in processing environments to prevent microbial growth. The LMF processing plants should minimize water use in production areas and promptly remove any leaks or condensation. In particular, wet sanitation should be avoided whenever possible, and if performed, surfaces must be dried immediately to prevent microbial growth (Beuchat et al., 2013; ICMSF, 2011).

The VBNC state is recognized as a microbial survival strategy under stresses such as dehydration, nutrient limitation, and sanitizer exposure (Balagurusamy et al., 2024; Kunadu et al., 2024). VBNC cells, although metabolically active and potentially pathogenic, do not form colonies under routine conditions and therefore may escape detection, leading to a false negative result (Foddai and Grant, 2020). Liu et al. (2023) proposed the term “viable cells with loss of culturability” to describe VBNC cells. The inability of VBNC cells to detoxify lethal free radicals either induced by the cells themselves or present in the culture medium is one of the main reasons for the non-culturability. This process may be due to the repression of periplasmic catalase, which breaks down toxic peroxide (Morishige et al., 2017). As a result, several proteins have been shown to play a significant role in the formation of VBNC cells; these include superoxide dismutase (SodA), catalases KatA and KatG, RNA polymerase sigma S (RpoS), alkyl hydroperoxide reductase subunit C (AhpC), sensory histidine kinase (EnvZ), and a LysRtype transcriptional regulator (OxyR) (İzgördü et al., 2022; Ma et al., 2024). In the current study, VBNC cells were defined as the population capable of resuscitation in the presence of catalase; however, no complementary assessments of metabolic activity or membrane integrity were conducted. According to our data, adaptation to DSB induced a

transition to the VBNC state, as evidenced by the resuscitate effect of catalase. The culturability increased between 1.1 and 2.8 log CFU/cm² for *Salmonella* and 0.6 to 2.2 log CFU/cm² for *C. sakazakii* after catalase treatment (VSC, Figures 1 and 2). This method has also been shown to successfully resuscitate *Salmonella* cells in the VBNC state following desiccation stress (Abdelhamid and Yousef, 2020; Morishige et al., 2017). Furthermore, T5 showed the largest differences between CSC and VSC for both species (Figures 1 and 2). The desiccation stress experienced by the bacteria following the brief hydrated phase (8 h) likely triggered defense mechanisms, resulting in a greater presence of VBNC cells in both pathogens. Lin et al. (2024) also suggested that a significant portion of the DSB population likely exists in the VBNC state. Thus, the occurrence of the VBNC state or injured cells in the LMF processing environment poses a considerable challenge to the validation of hygiene protocols. Routine verification of sanitation efficacy typically relies on conventional culture methods, which fail to detect bacteria in the VBNC state (Kazemzadeh-Narbat et al., 2021). Our data indicate that this limitation may lead to false-negative results during environmental monitoring, corroborating with Foddai and Grant (2020). Furthermore, they highlight the need for developing rapid and reliable detection methods capable of identifying VBNC cells, which can be integrated into routine monitoring within food manufacturing facilities.

The surface material only significantly impacted ($p<0.05$) the T5 protocol for both pathogens, with greater CSC counts on PP than SS (Figure 1 and 2). Factors such as surface roughness and hydrophobicity impact moisture retention and bacterial adhesion, influencing cell physiology (Ivers et al., 2024; Lehner et al., 2005). Hydrophobic materials like PP tend to promote the initial attachment of cells by reducing repulsive electrostatic interactions, while smoother and more hydrophilic surfaces such as stainless steel generally limit irreversible adhesion but may support more uniform film formation once attachment occurs (Carniello et al., 2018; Zhang et al., 2016; Wu et al., 2018). In addition, the DSB average thicknesses and the biomass of live and dead cells also varied according to the microorganism, surface type, and protocol, with values ranging from 3.3 to 12.7 µm and 29 to 92.2% (Table 3). However, it was not possible to establish a standard behavior of the DSB evaluated. In fact, it emphasizes the complex nature of biofilm formation, which depends on multiple environmental and

biological factors (Flemming et al., 2023; Sauer et al., 2022). In general, T1 resulted in greater surface coverage, reflecting more favorable conditions for microbial growth due to extended hydrated phase exposure (Figure 5 and 6). Interestingly, T3 (24-h wet + 72-h dry) produced the densest biofilm (except for *Salmonella* on SS), despite having similar microbial counts to T1 (Figure 1 and 2), suggesting an adaptive response to desiccation stress. Although T5 showed thickness close to T3, the spatial distribution (Figure 5 and 6) and the CSC counts (Figure 1 and 2) indicate a softer and less dense biofilm, emphasizing the critical influence of the hydrated phase on the DSB structure. Furthermore, *Salmonella* DSB showed more heterogeneous surface coverage and biomass thickness (Figure 5). Lin et al. (2024) similarly reported that *S.* Typhimurium DSB exhibited a heterogeneous vertical distribution with a thickness of around 15 μm. Capita et al. (2019) evaluated hydrated biofilms formed by *Salmonella* on polystyrene at 37 °C for 24 h, and obtained thicknesses between 15.7 and 53.3 μm. In contrast, *C. sakazakii* formed biofilms with more uniform spatial distribution across protocols (Figure 6), emphasizing greater adaptability and potential for biofilm formation under extreme conditions.

Previous studies describe DSB EPS as dense and compact, with fewer filaments compared to hydrated surface biofilms (WSB) (Lin et al., 2024; Rahman et al., 2022). The EPS matrix is vital for desiccation protection, by retaining moisture and shielding cells from physical and chemical damage, contributing to biofilm persistence in industrial settings (Greffe and Michiels, 2020; Iibuchi et al., 2010; Machado et al., 2012). In the current study, the presence of EPS was confirmed in all DSB by SEM, with filamentous EPS more prominent in *Salmonella* (Figure 3, green arrow). SEM imaging also revealed typical desiccation-related morphological changes in *Salmonella* and *C. sakazakii* cells, including cell lysis, reduced turgor pressure, and membrane damage (Figures 3 and 4). High intracellular osmolyte concentrations, produced in response to desiccation, drive water efflux; forcing bacteria to adopt energy-intensive mechanisms to maintain turgor (Esbelin et al., 2018). Although essential for survival, these adaptations are energetically costly. When osmolyte biosynthesis or uptake becomes too costly, energy depletion reduces turgor pressure (Craig et al., 2021). This combined energy and desiccation stress impairs cell division by inhibiting septation and inducing bacterial filamentation (Burgess et al., 2016;

Yan et al., 2024); observed in all evaluated DSB (Figures 3 and 4). Filamentation increases biomass without a corresponding increase in cell number, possibly reflecting an adaptive advantage or survival strategy. Stackhouse et al. (2012) reported that filamentation enhances desiccation tolerance. In addition, changes in cell shape, including a shift toward coccoid morphology (more frequent in *Salmonella* biofilms), may represent further structural adaptation to desiccation stress and may indicate a transition to the VBNC state (Ma et al., 2024). Dong et al. (2020) linked coccoid forms in VBNC *Salmonella* cells to cell wall alterations.

In conclusion, this study demonstrated that both *Salmonella* and *C. sakazakii* can form DSB on SS and PP even under moisture-limited conditions. The duration of the hydrated phase emerged as a critical factor influencing both the extent of biofilm formation and the induction of the VBNC state. In addition, *C. sakazakii* exhibited a greater capacity for DSB formation compared to *Salmonella*, suggesting higher adaptability to desiccation stress conditions. These findings emphasize the importance of strict hygiene and moisture control measures in LMF processing environments to prevent biofilm establishment and pathogen persistence. Furthermore, risk monitoring approaches that consider the induction of the VBNC state and the potential resurrection of these cells should be integrated into prerequisite programs and hazard analysis and critical control points (HACCP). Moreover, these data may contribute to risk assessment studies to establish more effective control measures for ensuring the safety of LMF. However, despite these relevant contributions, the study has some limitations, such as the use of a limited number of bacterial strains and surface types. Therefore, future studies assessing the long-term survival of DSB, as well as their resistance to both dry and wet sanitizers routinely applied in the food industry across different surface types are needed. In addition, transcriptomic analysis to determine mechanisms involved in transition to VBNC in DSB shall be investigated.

CRediT authorship contribution statement

Vinícius S. A. Vaz: Writing – original draft, Visualization, Investigation, Formal analysis, Data curation. **Jéssica de A.F.F. Finger:** Writing – original draft, Visualization, Formal analysis, Data curation. **Raul F. Pereira:** Methodology, Investigation, Formal analysis. **Mariana S. Derami:** Visualization, Investigation.

Jean-Yves Maillard: Methodology, Writing – review & editing**. Maristela S. Nascimento:** Writing – review & editing, Resources, Project administration, Methodology, Funding acquisition, Conceptualization, Data curation.

Declaration of competing interest

The authors declare that they have no known competing financial interests or personal relationships that could have appeared to influence the work reported in this paper.

Acknowledgements

The authors acknowledge financial support from Fundação de Amparo à Pesquisa do Estado de São Paulo (FAPESP; 2021/06809-2 and 2023/03076-0), Conselho Nacional de Desenvolvimento Científico e Tecnológico (CNPq; 305702/2021-1), and Coordenação de Aperfeiçoamento de Pessoal de Nível Superior – Brazil (CAPES; Finance Code 001). The authors also thank the National Institute of Science and Technology on Photonics Applied to Cell Biology (INFABIC) at the State University of Campinas for providing access to CLSM equipment and technical support (FAPESP; 2014/50938-8 and CNPq; 465699/2014-6).

References

Abdallah, M., Benoliel, C., Drider, D., Dhulster, P., Chihib, N. E., 2014. Biofilm formation and persistence on abiotic surfaces in the context of food and medical environments. *Arch. Microbiol.* 196, 453-472. https://doi.org/10.1007/s00203-014-0983-1.

Abdelhamid, A. G., Yousef, A. E., 2020. Collateral adaptive responses induced by desiccation stress in *Salmonella* enterica. *LWT* 133, 110089. https://doi.org/10.1016/j.lwt.2020.110089.

Akuzov, D., Brümmer, F., Vladkova, T., 2013. Some possibilities to reduce the biofilm formation on transparent siloxane coatings. *Colloids Surf. B: Biointerfaces* 104, 303-310. https://doi.org/10.1016/j.colsurfb.2012.09.036.

Almatroudi A, Hu H, Deva A, Gosbell IB, Jacombs A, Jensen SO, *et al*. A new dry-surface biofilm model: An essential tool for efficacy testing of hospital surface decontamination procedures. *J Microbiol Methods.* 2015; **117**:171–176.

564 Alonso, V. P. P., Gonçalves, M. P. M., de Brito, F. A. E., Barboza, G. R.,
565 Rocha, L. D. O., Silva, N. C. C., 2023. Dry surface biofilms in the food processing
566 industry: An overview on surface characteristics, adhesion and biofilm formation,
567 detection of biofilms, and dry sanitization methods. *Compr. Rev. Food Sci. Food*
568 *Saf.* 22, 688-713. https://doi.org/10.1111/1541-4337.13089.
569 Alvarez-Ordóñez, A., Coughlan, L. M., Briandet, R., Cotter, P. D., 2019.
570 Biofilms in food processing environments: challenges and opportunities. *Annu.*
571 *Rev. Food Sci. Technol.* 10, 173-195. https://doi.org/10.1146/annurev-food-
572 032818-121805.
573 Amaeze, N., Akinbobola, A. B., Kean, R., Ramage, G., Williams, C.,
574 Mackay, W., 2024. Transfer of microorganisms from dry surface biofilms and the
575 influence of long survival under conditions of poor nutrition and moisture on the
576 virulence of *Staphylococcus aureus*. *J. Hosp. Infect.* 150, 34-39.
577 https://doi.org/10.1016/j.jhin.2024.03.023.
578 Anderson, D., Anderson, N., Harris, L. J., Ocasio, W., 2017. Validation
579 Requirements in Heat-Processed Low-Moisture Foods. In: *Control of Salmonella*
580 *and Other Bacterial Pathogens in Low Moisture Foods*, pp. 149–173.
581 https://doi.org/10.1002/9781119071051.CH7.
582 Balagurusamy, R., Gopi, L., Kumar, D. S. S., Viswanathan, K.,
583 Meganathan, V., Sathiyamurthy, K., Athmanathan, B., 2024. Significance of
584 Viable But Non-culturable (VBNC) state in vibrios and other pathogenic bacteria:
585 induction, detection and the role of resuscitation promoting factors (Rpf). *Curr.*
586 *Microbiol.* 81, 417. https://doi.org/10.1007/s00284-024-03947-8.
587 Beuchat, L. R., Komitopoulou, E., Beckers, H., Betts, R. P., Bourdichon,
588 F., Fanning, S., ..., Ter Kuile, B. H., 2013. Low-water activity foods: increased
589 concern as vehicles of foodborne pathogens. *J. Food Prot.* 76, 150-172.
590 https://doi.org/10.4315/0362-028X.JFP-12-211.
591 Borisov, V. B., Siletsky, S. A., Nastasi, M. R., Forte, E., 2021. ROS
592 defense systems and terminal oxidases in bacteria. *Antioxidants* 10, 839.
593 https://doi.org/10.3390/antiox10060839.
594 Burgess, C. M., Gianotti, A., Gruzdev, N., Holah, J., Knøchel, S., Lehner,
595 A., ..., Tresse, O., 2016. The response of foodborne pathogens to osmotic and
596 desiccation stresses in the food chain. *Int. J. Food Microbiol.* 221, 37-53.
597 https://doi.org/10.1016/j.ijfoodmicro.2015.12.014.

598 Cámara, M., Green, W., MacPhee, C. E., Rakowska, P. D., Raval, R.,
599 Richardson, M. C., ..., Webb, J. S., 2022. Economic significance of biofilms: a
600 multidisciplinary and cross-sectoral challenge. *NPJ Biofilms Microbiomes* 8, 42.
601 https://doi.org/10.1038/s41522-022-00306-y.
602 Capita, R., Fernández-Pérez, S., Buzón-Durán, L., Alonso-Calleja, C.,
603 2019. Effect of sodium hypochlorite and benzalkonium chloride on the structural
604 parameters of the biofilms formed by ten *Salmonella* enterica serotypes.
605 *Pathogens* 8, 154. http://dx.doi.org/10.3390/pathogens8030154.
606 Carniello, V., Peterson, B. W., van der Mei, H. C., Busscher, H. J., 2018.
607 Physico-chemistry from initial bacterial adhesion to surface-programmed biofilm
608 growth. *Adv. Colloid Interface Sci.* 261, 1-14.
609 https://doi.org/10.1016/j.cis.2018.10.005.
610 Centeleghe, I., Norville, P., Hughes, L., Maillard, J. Y. 2023. *Klebsiella*
611 *pneumoniae* survives on surfaces as a dry biofilm. *American Journal of Infection*
612 *Control* 51, 1157-1162. https://doi.org/10.1016/j.ajic.2023.02.009.
613 Chaggar, G. K., Bryant, D. B., Chen, R., Fajardo, D., Jules-Culver, Z. A.,
614 Drolia, R., Oliver, H. F., 2024. Development *of Salmonella* enterica serovar
615 Typhimurium, *Listeria monocytogenes*, and *Pseudomonas aeruginosa* multi-
616 species in vitro dry surface biofilm models: Insights into resilience and
617 persistence in low-moisture environments. *Food Control* 166, 110703.
618 https://doi.org/10.1016/j.foodcont.2024.110703.
619 Chen, G., Lin, M., Chen, Y., Xu, W., Zhang, H., 2021. Induction of a viable
620 but nonculturable state, thermal and sanitizer tolerance, and gene expression
621 correlation with desiccation-adapted biofilm and planktonic Salmonella in
622 powdered infant formula. *J. Food Prot.* 84, 1194-1201.
623 Chowdhury, D., Tahir, S., Legge, M., Hu, H., Prvan, T., Johani, K., ... ,
624 Vickery, K., 2018. Transfer of dry surface biofilm in the healthcare environment:
625 the role of healthcare workers' hands as vehicles. *J. Hosp. Infect.* 100, e85-e90.
626 https://doi.org/10.1016/j.jhin.2018.06.021.
627 Codex Alimentarius, 2018. Code of Hygienic Practice for Low-Moisture
628 Foods. CXC 75-2015. https://www.fao.org/fao-who-
629 codexalimentarius/codextexts/codes-of-practice/en/ (accessed 21 February
630 2025).
631 Craig, K., Johnson, B. R., Grunden, A., 2021. Leveraging *Pseudomonas*

stress response mechanisms for industrial applications. *Front. Microbiol.* 12, 660134. https://doi.org/10.3389/fmicb.2021.660134.

Dallal, M. M. S., Kelishomi, F. Z., Nikkhahi, F., Salehi, T. Z., Fardsanei, F., Peymani, A., 2023. Biofilm formation, antimicrobial resistance genes, and genetic diversity of *Salmonella* enterica subspecies enterica serotype Enteritidis isolated from food and animal sources in Iran. *J. Glob. Antimicrob. Resist.* 34, 240-246. https://doi.org/10.1016/j.jgar.2023.08.004.

Dass, S. C., Wang, R., 2022. Biofilm through the looking glass: A microbial food safety perspective. *Pathogens* 11, 346. https://doi.org/10.3390/pathogens11030346.

Dong, K., Pan, H., Yang, D., Rao, L., Zhao, L., Wang, Y., Liao, X., 2020. Induction, detection, formation, and resuscitation of viable but non-culturable state microorganisms. *Compr. Rev. Food Sci. Food Saf.* 19, 149-183. https://doi.org/10.1111/1541-4337.12513.

Duggan, K., Shepherd, M., Maillard, J. Y., 2024. Susceptibility of *Salmonella* enterica Typhimurium dry surface biofilms to disinfection. *J. Food Saf.* 44, e13117. https://doi.org/10.1111/jfs.13117.

Eriksson de Rezende, C. L., Mallinson, E. T., Gupte, A., Joseph, S. W. 2001. *Salmonella* spp. are affected by different levels of water activity in closed microcosms. *J. Ind. Microbiol. Biotechnol.* 26, 222-225. https://doi.org/10.1038/sj.jim.7000116.

Esbelin, J., Santos, T., Hébraud, M., 2018. Desiccation: an environmental and food industry stress that bacteria commonly face. *Food Microbiol.* 69, 82-88. https://doi.org/10.1016/j.fm.2017.07.017.

Esther C, Olive C, Louisin M, Dramé M, Marion-Sanchez K. A new spray-based method for the in-vitro development of dry-surface biofilms. *Microbiol Open.* 2023; **12**:e1330.

FAO/WHO, 2006. *Enterobacter sakazakii* and *Salmonella* in powdered infant formula. Microbiological Risk Assessment Series No. 10. Rome. 52. https://www.who.int/publications/i/item/9241563311.

Flemming, H. C., van Hullebusch, E. D., Neu, T. R., Nielsen, P. H., Seviour, T., Stoodley, P., ..., Wuertz, S., 2023. The biofilm matrix: multitasking in a shared space. *Nat. Rev. Microbiol.* 21, 70-86. https://doi.org/10.1038/s41579-022-00791-0.

Foddai, A. C., Grant, I. R., 2020. Methods for detection of viable foodborne pathogens: Current state-of-art and future prospects. *Appl. Microbiol. Biotechnol.* 104, 4281-4288. https://doi.org/10.1007/s00253-020-10542-x.

Galié, S., García-Gutiérrez, C., Miguélez, E. M., Villar, C. J., Lombó, F., 2018. Biofilms in the food industry: health aspects and control methods. *Front. in Microbiol.* 9, 1-18. https://doi.org/10.3389/fmicb.2018.00898.

Greffe, V. R. G., Michiels, J., 2020. Desiccation-induced cell damage in bacteria and the relevance for inoculant production. *Appl. Microbiol. Biotechnol.* 104, 3757–3770. https://doi.org/10.1007/s00253-020-10501-6

Gruzdev, N., McClelland, M., Porwollik, S., Ofaim, S., Pinto, R., Saldinger-Sela, S., 2012. Global transcriptional analysis of dehydrated *Salmonella* enterica serovar Typhimurium. *Appl. Environ. Microbiol.* 78, 7866-7875. https://doi.org/10.1128/aem.01822-12.

Han, L., Wang, K., Ma, L., Delaquis, P., Bach, S., Feng, J., Lu, X., 2020. Viable but nonculturable *Escherichia coli* O157: H7 and *Salmonella* enterica in fresh produce: Rapid determination by loop-mediated isothermal amplification coupled with a propidium monoazide treatment. *Appl. Environ. Microbiol.* 86, e02566-19. https://doi.org/10.1128/AEM.02566-19.

Heydorn, A., Nielsen, A. T., Hentzer, M., Sternberg, C., Givskov, M., Ersbøll, B. K., Molin, S. 2000. Quantification of biofilm structures by the novel computer program COMSTAT. *Microbiology* 146, 2395-2407. https://doi.org/10.1099/00221287-146-10-2395.

Iibuchi, R., Hara-Kudo, Y., Hasegawa, A., Kumagai, S., 2010. Survival of *Salmonella* on a polypropylene surface under dry conditions in relation to biofilm-formation capability. *J. Food Prot.* 73, 1506-1510. https://doi.org/10.4315/0362-028X-73.8.1506.

International Commission on Microbiological Specifications for Foods (ICMSF), 2011. *Microorganisms in Foods 8: Use of Data for Assessing Process Control and Product Acceptance*. Springer. ISBN 978-1-4419-9373-1.

Ivers, C., Kaya, E. C., Yucel, U., Boyle, D., Trinetta, V., 2024. Evaluation of *Salmonella* biofilm attachment and hydrophobicity characteristics on food contact surfaces. *BMC Microbiol.* 24, 387. https://doi.org/10.1186/s12866-024-03556-2.

699 İzgördü, Ö. K., Darcan, C., Kariptaş, E., 2022. Overview of VBNC, a
700 survival strategy for microorganisms. *3 Biotech* 12, 307.
701 https://doi.org/10.1007/s13205-022-03371-4.
702 Karygianni, L., Ren, Z., Koo, H., Thurnheer, T., 2020. Biofilm matrixome:
703 extracellular components in structured microbial communities. *Trends Microbiol.*
704 28, 668-681. https://doi.org/10.1016/j.tim.2020.03.016
705 Kazemzadeh-Narbat, M., Cheng, H., Chabok, R., Alvarez, M. M., De La
706 Fuente-Nunez, C., Phillips, K. S., Khademhosseini, A., 2021. Strategies for
707 antimicrobial peptide coatings on medical devices: A review and regulatory
708 science perspective. *Crit. Rev. Biotechnol.* 41, 94-120.
709 https://doi.org/10.1080/07388551.2020.1828810.
710 Kunadu, A. P. H., Nyamekye, M. A., Gosu-Attapkah, C., 2024. Bacteria
711 stress adaptation: Implication and control. In O. A. Ijabadeniyi and O. F. Olagunju
712 (Eds.), *Food safety and toxicology: Present and future perspectives*, Berlin: De
713 Gruyter, pp. 127–148. https://doi.org/10.1515/9783110748345-006.
714 Learbuch, K. L. G., Lut, M. C., Liu, G., Smidt, H., van der Wielen, P. W. J.
715 J., 2019. Legionella growth potential of drinking water produced by a reverse
716 osmosis pilot plant. *Water Res.* 157, 55-63.
717 https://doi.org/10.1016/j.waters.2019.03.037.
718 Ledwoch, K., Dancer, S. J., Otter, J. A., Kerr, K., Roposte, D., Rushton, L.,
719 ... , Maillard, J. Y., 2018. Beware biofilm! Dry biofilms containing bacterial
720 pathogens on multiple healthcare surfaces; a multi-centre study. *J. Hosp. Infect.*
721 100, e47-e56. https://doi.org/10.1016/j.jhin.2018.06.028.
722 Ledwoch, K., Said, J., Norville, P., Maillard, J. Y., 2019. Artificial dry
723 surface biofilm models for testing the efficacy of cleaning and disinfection. *Lett.*
724 *Appl. Microbiol.* 68, 329-336. https://doi.org/10.1111/lam.13143.
725 Ledwoch, K., Vickery, K., Maillard, J. Y., 2022. Dry surface biofilms: what
726 you need to know. *Br. J. Hosp. Med.* 83, 1-3.
727 https://doi.org/10.12968/hmed.2022.0274.
728 Lee, H., Beuchat, L. R., Ryu, J. H., Kim, H., 2018. Inactivation of
729 *Salmonella* Typhimurium on red chili peppers by treatment with gaseous chlorine
730 dioxide followed by drying. *Food Microbiol.* 76, 78-82.
731 https://doi.org/10.1016/j.fm.2018.04.016.
732 Lehner, A., Riedel, K., Eberl, L., Breeuwer, P., Diep, B., Stephan, R., 2005.

733 Biofilm formation, extracellular polysaccharide production, and cell-to-cell
734 signaling in various *Enterobacter* sakazakii strains: aspects promoting
735 environmental persistence. *J. Food Prot.* 68, 2287-2294.
736 https://doi.org/10.4315/0362-028X-68.11.2287.
737 Lin, Z., Liang, Z., He, S., Chin, F. W. L., Huang, D., Hong, Y., ..., Li, D.,
738 2024. *Salmonella* dry surface biofilm: morphology, single-cell landscape, and
739 sanitization. *Appl. Environ. Microbiol.* 90, e01623-24.
740 https://doi.org/10.1128/aem.01623-24.
741 Liu, J., Yang, L., Kjellerup, B. V., Xu, Z., 2023. Viable but nonculturable
742 (VBNC) state, an underestimated and controversial microbial survival strategy.
743 *Trends Microbiol.* 31, 1013-1023. https://doi.org/10.1016/j.tim.2023.04.009.
744 Liu, S., Roopesh, M. S., Tang, J., Wu, Q., Qin, W., 2022. Recent
745 development in low-moisture foods: Microbial safety and thermal process. *Food*
746 *Res. Int.* 155, 111072. https://doi.org/10.1016/j.foodres.2022.111072.
747 Lories, B., Belpaire, T. E., Yssel, A., Ramon, H., Steenackers, H. P., 2020.
748 Agaric acid reduces *Salmonella* biofilm formation by inhibiting flagellar motility.
749 *Biofilm* 2, 100022. https://doi.org/10.1016/j.bioflm.2020.100022.
750 Lou, Z., Song, X., Hong, Y., Wang, H., Lin, Y., 2013. Separation and
751 enrichment of burdock leaf components and their inhibition activity on biofilm
752 formation of *E. coli*. *Food Control* 32, 270-274.
753 https://doi.org/10.1016/j.foodcont.2012.11.020.
754 Ly, V., Parreira, V. R., Farber, J. M., 2019. Current understanding and
755 perspectives on *Listeria monocytogenes* in low-moisture foods. *Curr. Opin. Food*
756 *Sci.* 26, 18-24. https://doi.org/10.1016/j.cofs.2019.02.012.
757 Highmore, C. J., Warner, J. C., Rothwell, S. D., Wilks, S. A., Keevil, C. W.,
758 2018. Viable-but-nonculturable *Listeria monocytogenes* and *Salmonella* enterica
759 serovar Thompson induced by chlorine stress remain infectious. *MBio* 9, 10-
760 1128. https://doi.org/10.1128/mbio.00540-18.
761 Ma, Z., Xu, W., Li, S., Chen, S., Yang, Y., Li, Z., ... , Zhang, H., 2024. Effect
762 of RpoS on the survival, induction, resuscitation, morphology, and gene
763 expression of viable but non-culturable *Salmonella* Enteritidis in powdered infant
764 formula. *Int. J. Food Microbiol.* 410, 110463.
765 https://doi.org/10.1016/j.ijfoodmicro.2023.110463.

766 Machado, I., Lopes, S. P., Sousa, A. M., Pereira, M. O., 2012. Adaptive
767 response of single and binary *Pseudomonas aeruginosa* and *Escherichia coli*
768 biofilms to benzalkonium chloride. *J. Basic Microbiol.* 52, 43-52.
769 https://doi.org/10.1002/jobm.201100137.
770 Maćkiw, E., Kowalska, J., Korsak, D., Stasiak, M., Antoszewska, A.,
771 Ławrynowicz-Paciorek, M., Postupolski, J., 2024. Thermal resistance of selected
772 strains of *Salmonella* spp. isolated from eggs and sesame seeds. *LWT* 198,
773 115907. https://doi.org/10.1016/j.lwt.2024.115907.
774 Morishige, Y., Koike, A., Tamura-Ueyama, A., Amano, F., 2017. Induction
775 of viable but nonculturable *Salmonella* in exponentially grown cells by exposure
776 to a low-humidity environment and their resuscitation by catalase. *J. Food Prot.*
777 80, 288-294. https://doi.org/10.4315/0362-028x.jfp-16-183.
778 Nascimento, M. S., Carminati, J. A., Silva, I. C. R. N., Silva, D. L., Bernardi,
779 A. O., Copetti, M. V., 2018. *Salmonella*, *Escherichia coli* and *Enterobacteriaceae*
780 in the peanut supply chain: From farm to table. *Food Res. Int.* 105, 930-935.
781 https://doi.org/10.1016/j.foodres.2017.12.021.
782 Pan, H., Ren, Q., 2022. Wake up! Resuscitation of viable but nonculturable
783 bacteria: mechanism and potential application. *Foods* 12, 82.
784 https://doi.org/10.3390/foods12010082.
785 Rahman, M. A., Amirkhani, A., Parvin, F., Chowdhury, D., Molloy, M. P.,
786 Deva, A. K., Vickery, K., Hu, H., 2022. One Step Forward with Dry Surface Biofilm
787 (DSB) of *Staphylococcus aureus*: TMT-Based Quantitative Proteomic Analysis
788 Reveals Proteomic Shifts between DSB and Hydrated Biofilm. *Int. J. Mol. Sci.* 23,
789 12238. https://doi.org/10.3390/ijms232012238.
790 Rodrigues, C. M., Takita, M. A., Coletta-Filho, H. D., Olivato, J. C.,
791 Caserta, R., Machado, M. A., De Souza, A. A., 2008. Copper resistance of biofilm
792 cells of the plant pathogen *Xylella fastidiosa*. *App. Microbiol. Biotechnol.* 77,
793 1145-1157. https://doi.org/10.1007/s00253-007-1232-1.
794 Rosado, M. S., 2009. Biofilme de *Enterococcus faecium* em superfície de
795 aço inoxidável: caracterização tecnológica, modelagem e controle por agentes
796 sanitizantes. Dissertação (Mestre em Tecnologia de Alimentos) - Faculdade de
797 Engenharia de Alimentos, Universidade Estadual de Campinas, Campinas (SP),
798 84p.

Sadiq, F. A., De Reu, K., Burmølle, M., Maes, S., Heyndrickx, M., 2023. Synergistic interactions in multispecies biofilm combinations of bacterial isolates recovered from diverse food processing industries. *Front. Microbiol.* 14, 1159434. https://doi.org/10.3389/fmicb.2023.1159434.

Salive, A. F. V., Prudêncio, C. V., Baglinière, F., Oliveira, L. L., Ferreira, S. O., Vanetti, M. C. D., 2020. Comparison of stress conditions to induce viable but non-cultivable state in *Salmonella*. *Braz. J. Microbiol.* 51, 1269-1277. https://doi.org/10.1007/s42770-020-00261-w.

Sauer, K., Stoodley, P., Goeres, D. M., Hall-Stoodley, L., Burmølle, M., Stewart, P. S., Bjarnsholt, T., 2022. The biofilm life cycle: expanding the conceptual model of biofilm formation. *Nat. Rev. Microbiol.* 20, 608-620. https://doi.org/10.1038/s41579-022-00767-0.

Sawale, M., Ozadali, F., Valentine, C. J., Benyathiar, P., Drolia, R., Mishra, D. K., 2022. Impact of bovine lactoferrin fortification on pathogenic organisms to attenuate the risk of infection for infants. *Food Control* 139, 109078. https://doi.org/10.1016/j.foodcont.2022.109078.

Stackhouse, R. R., Faith, N. G., Kaspar, C. W., Czuprynski, C. J., Wong, A. C., 2012. Survival and virulence of *Salmonella* enterica serovar enteritidis filaments induced by reduced water activity. *App. Environ. Microbiol.* 78, 2213–2220. https://doi.org/10.1128/aem.06774-11.

Strysko, J., Cope, J. R., Martin, H., Tarr, C., Hise, K., Collier, S., Bowen, A., 2020. Food safety and invasive *Cronobacter* infections during early infancy, 1961–2018. *Emerg. Infect. Dis.* 26, 857. https://doi.org/10.3201/eid2605.190858.

Umeda, N. S., de Filippis, I., Forsythe, S. J., Brandão, M. L. L., 2017. Phenotypic characterization of *Cronobacter* spp. strains isolated from foods and clinical specimens in Brazil. *Food Res. Int.* 102, 61-67. https://doi.org/10.1016/j.foodres.2017.09.083.

Vickery, K., Deva, A., Jacombs, A., Allan, J., Valente, P., Gosbell, I. B., 2012. Presence of biofilm containing viable multiresistant organisms despite terminal cleaning on clinical surfaces in an intensive care unit. *J. Hosp. Infect.* 80, 52-55. https://doi.org/10.1016/j.jhin.2011.07.007.

von Hertwig, A. M., Neto, D. P. A., de Almeida, E. A., Casas, M. R. T., do Nascimento, M. D. S., 2019. Genetic diversity, antimicrobial resistance and virulence profile of *Salmonella* isolated from the peanut supply chain.

International *J. Food Microbiol.* 294, 50-54. DOI: 10.1016/j.ijfoodmicro.2019.02.005.

von Hertwig, A. M., Prestes, F. S., Nascimento, M. S., 2022. Biofilm formation and resistance to sanitizers by *Salmonella* spp. Isolated from the peanut supply chain. *Food Res. Int.* 152, 110882. https://doi.org/10.1016/j.foodres.2021.110882.

Vorregaard, M. 2008. *Comstat2-a modern 3D image analysis environment for biofilms* (Master's thesis, Technical University of Denmark, DTU, DK-2800 Kgs. Lyngby, Denmark).

Wang, Z., Zhu, T., Chen, Z., Meng, J., Simpson, D. J., Gänzle, M. G., 2021. Genetic determinants of stress resistance in desiccated *Salmonella* enterica. *Appl. Environ. Microbiol.* 87, e01683-21. https://doi.org/10.1128/aem.01683-21.

Weber, D. J., Rutala, W. A., Anderson, D. J., Sickbert-Bennett, E. E., 2023. Biofilms on medical instruments and surfaces: Do they interfere with instrument reprocessing and surface disinfection. *Am. J. Infect. Control* 51, A114-A119. https://doi.org/10.1016/j.ajic.2023.04.158.

Wu, S., Altenried, S., Zogg, A., Zuber, F., Maniura-Weber, K., Ren, Q., 2018. Role of the surface nanoscale roughness of stainless steel on bacterial adhesion and microcolony formation. *ACS omega* 3, 6456-6464. https://doi.org/10.1021/acsomega.8b00769.

Yan, Y., Cao, M., Ma, J., Suo, J., Bai, X., Ge, W., ..., Yang, B., 2024. Mechanisms of thermal, acid, desiccation and osmotic tolerance of *Cronobacter* spp. *Crit. Rev. Food Sci. Nutr.* 1-23. https://doi.org/10.1080/10408398.2024.2447304.

Zhang, X. H., Ahmad, W., Zhu, X. Y., Chen, J., Austin, B., 2021. Viable but nonculturable bacteria and their resuscitation: implications for cultivating uncultured marine microorganisms. *MLST* 3, 189-203. https://doi.org/10.1007/s42995-020-00041-3.

Zhang, G., Wang, H., Chen, S., Yang, X., Xie, W., He, Y., 2016. Effect of tribocharger material on the triboelectric characteristics of coal and mineral particles. *Particul. Sci. Technol.* 35, 583-588. https://doi.org/10.1080/02726351.2016.1184729.

Ziech, R., Perin, A. P., Lampugnani, C., Serreno, M. J., Viana, C., Soares, V. M., Pereira, J. G., Pinto, J. P. A. N., Bersot, L. S., 2016. Biofilm-producing

867 ability and tolerance to industrial sanitizers in *Salmonella* spp. isolated from
868 Brazilian poultry processing plants. *LWT* 68.
869 https://doi.org/10.1016/j.lwt.2015.12.021.

FIGURE CAPTIONS

Figure 1. Counts of culturable sessile cells (CSC) and viable sessile cells (VSC) of *Salmonella* spp. dry surface biofilms (DSB) formed on stainless steel (SS) and polypropylene (PP) under protocols T1–T5: T1 (48 h wet/48 h dry), T2 (24 h wet/48 h dry), T3 (24 h wet/72 h dry), T4 (24 h wet/120 h dry), and T5 (8 h wet/48 h dry).

Figure 2. Counts of culturable sessile cells (CSC) and viable sessile cells (VSC) of *C. sakazakii* dry surface biofilms (DSB) formed on stainless steel (SS) and polypropylene (PP) under protocols T1 (48 h wet/48 h dry), T3 (24 h wet/72 h dry), T4 (24 h wet/120 h dry), and T5 (8 h wet/48 h dry).

Figure 3. Morphological changes in *Salmonella* cells in dry surface biofilms (DSB). Images correspond to protocols: (A) T1 – PP (48 h wet/48 h dry), (B) T2 – PP (24 h wet/48 h dry), (C) T3 – PP (24 h wet/72 h dry), (D) T4 – PP (24 h wet/120 h dry), and (E) T5 – SS (8 h wet/48 h dry). Yellow arrows indicate cell elongation, red arrows indicate cells showing wrinkling/loss of turgor, blue arrows indicate coccoid forms, green arrows indicate extracellular polymeric substances (EPS) formation, and orange arrows indicate lysed cells.

Figure 4. Morphological changes in *C. sakazakii* cells in dry surface biofilms (DSB). Images correspond to protocols: (A) T1 – PP (48 h wet/48 h dry), (B) T3 – SS (24 h wet/72 h dry), (C) T4 – PP (24 h wet/120 h dry), and (D) T5 – SS (8 h wet/48 h dry). Yellow arrows indicate cell elongation, red arrows indicate cells showing wrinkling/loss of turgor, blue arrows indicate coccoid forms, green arrows indicate extracellular polymeric substances (EPS) formation, and orange arrows indicate lysed cells.

Figure 5. Three-dimensional surface plot of dry surface biofilms (DSB) formed by *Salmonella* on stainless steel (SS) and polypropylene (PP) under different protocols (wet phase/dry phase): T1 (48 h wet/48 h dry), T2 (24 h wet/48 h dry), T3 (24 h wet/72 h dry), T4 (24 h wet/120 h dry), and T5 (8 h wet/48 h dry). Includes mean height (3 points), standard deviation, and thickest point. Dark-colored regions indicate absence of cells; light-colored regions indicate presence. X and Y axes (μm); Z axis (intensity).

Figure 6. Three-dimensional surface plot of dry surface biofilms (DSB) formed by *C. sakazakii* on stainless steel (SS) and polypropylene (PP) under different protocols (wet phase/dry phase): T1 (48 h wet/48 h dry), T3 (24 h wet/72 h dry), T4 (24 h wet/120 h dry), and T5 (8 h wet/48 h dry). Includes mean height (3 points), standard deviation, and thickest point. Dark-colored regions indicate absence of cells; light colors indicate presence. X and Y axes (μm); Z axis (intensity).

Salmonella

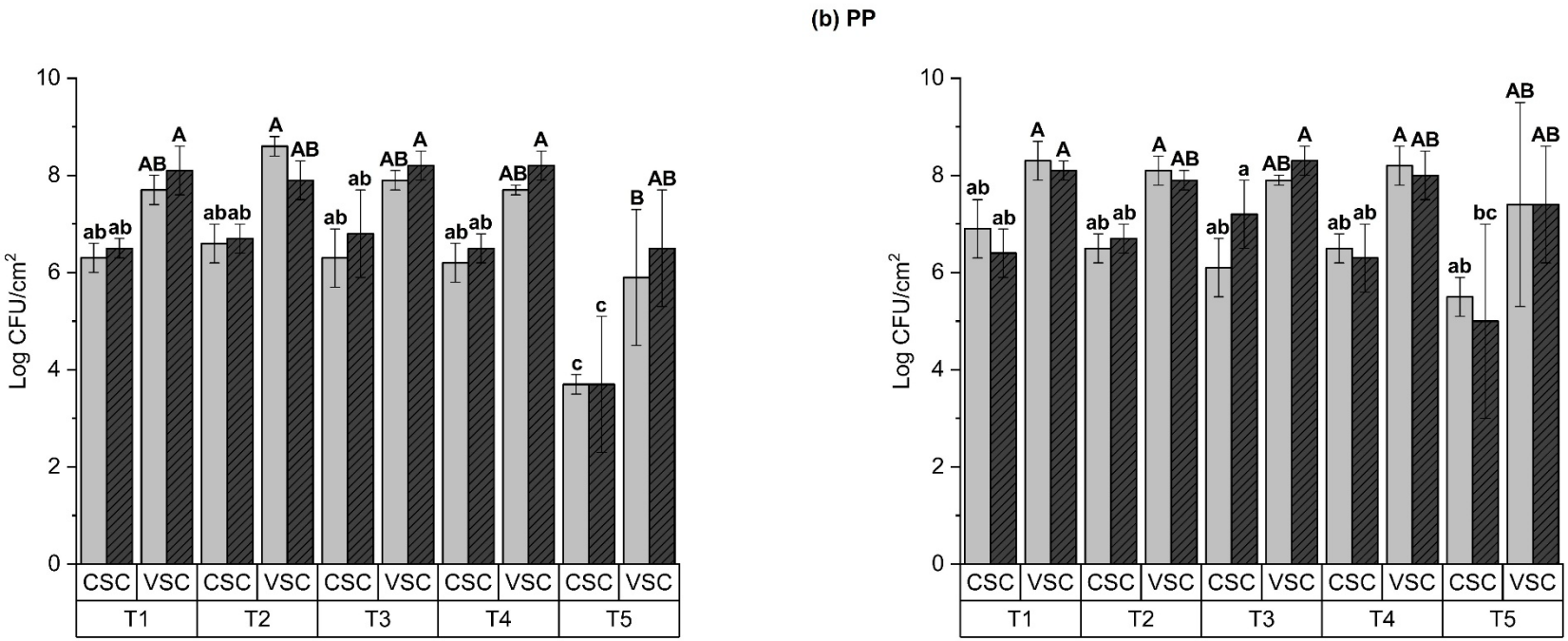

Figure 1

Cronobacter

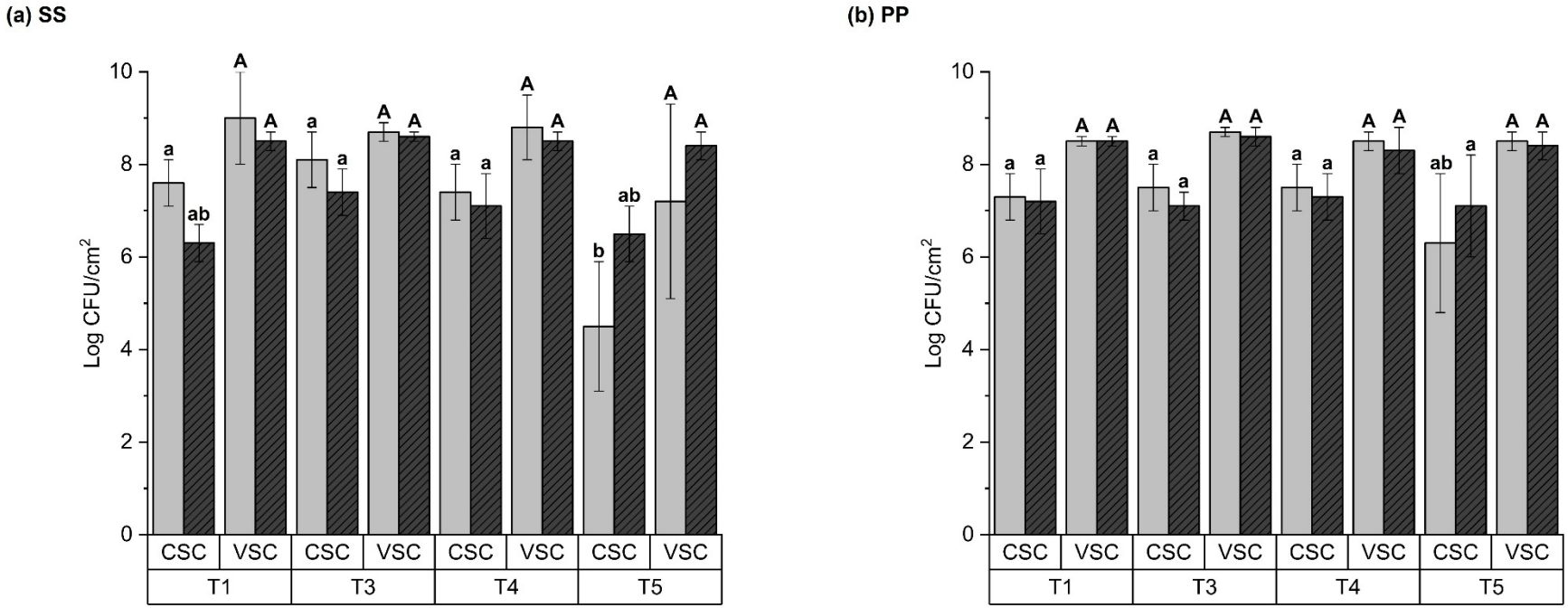

Figure 2

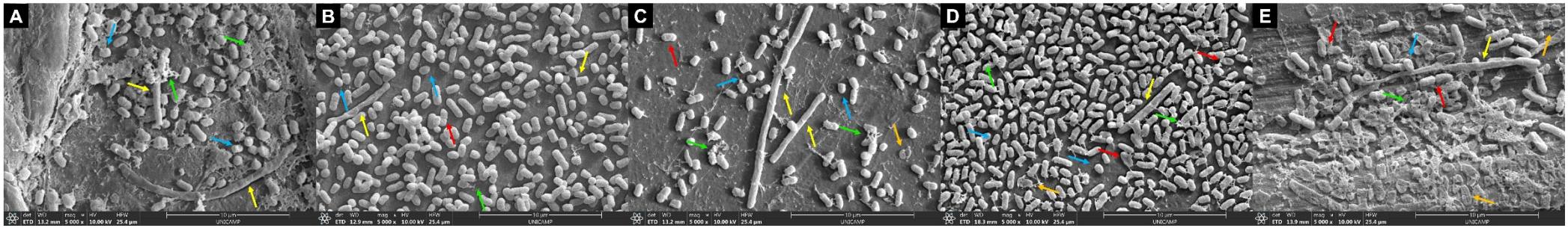

FIGURE 3

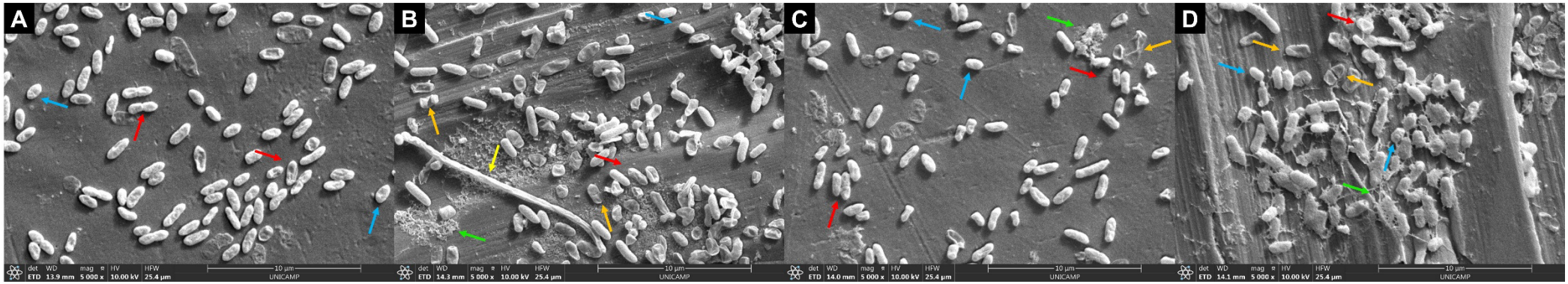

FIGURE 4

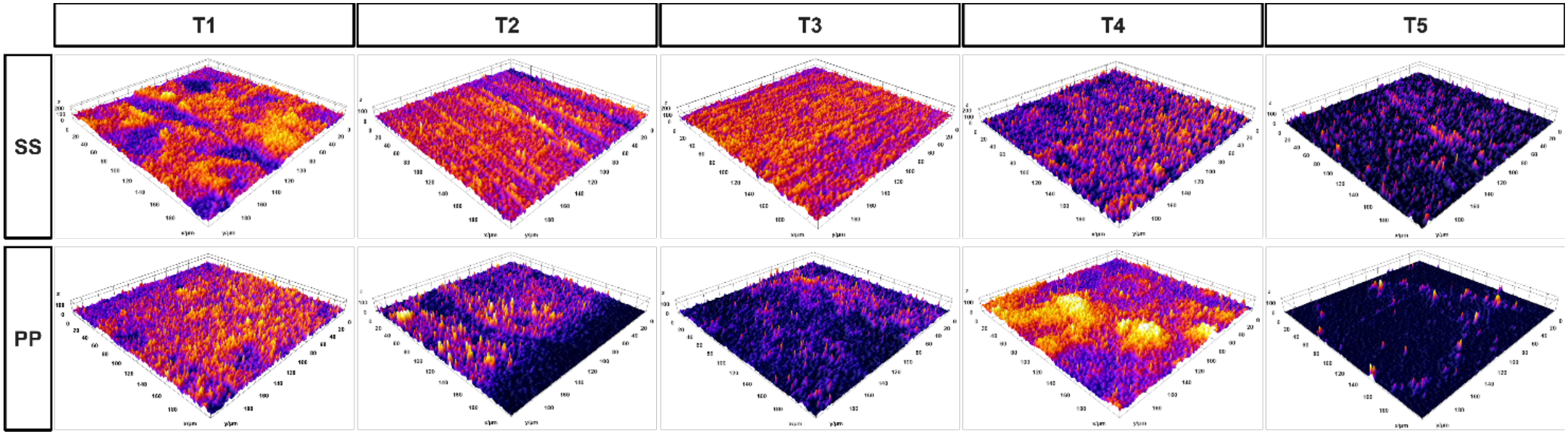

Figure 5

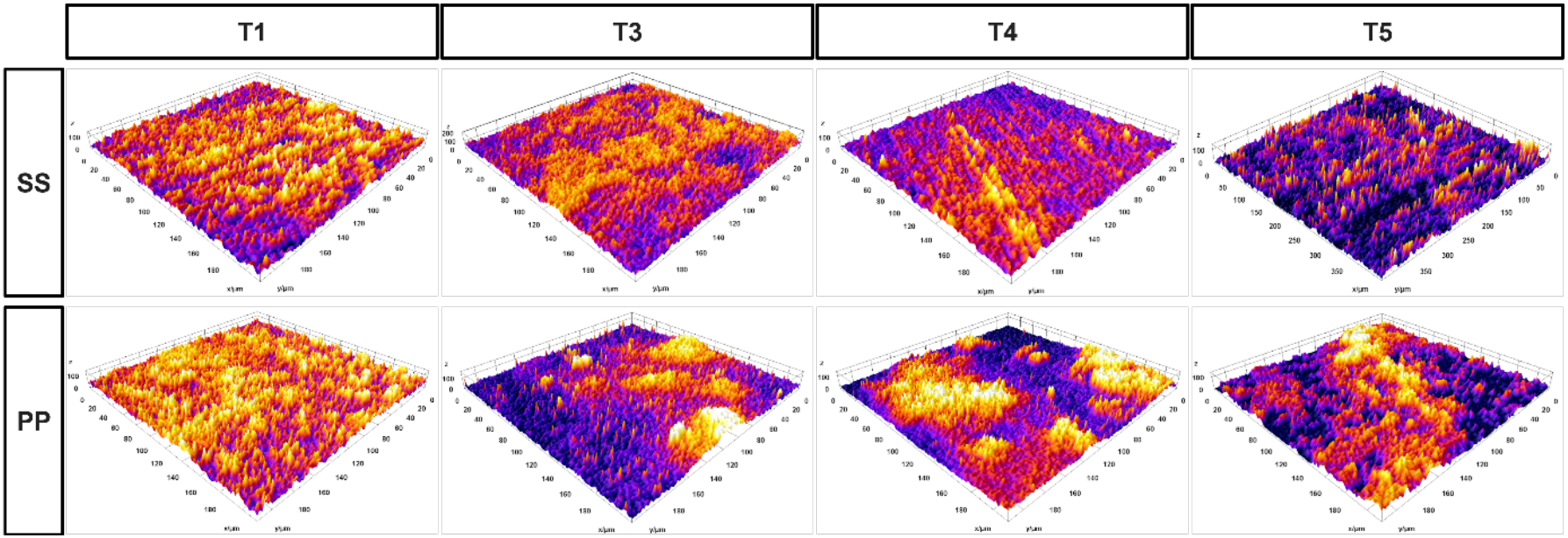

Figure 6